ISSN 1068-3666, Journal of Friction and Wear, 2013, Vol. 34, No. 2, pp. 114–119. © Allerton Press, Inc., 2013.
Original Russian Text © B. Jeremic, D. Vukelic, P.M. Todorovic, I. Macuzic, M. Pantic, D. Dzunic, B. Tadic, 2013, published in Trenie i Iznos, 2013, Vol. 34, No. 2, pp. 146–153.

Static Friction at High Contact Temperatures and Low Contact Pressure

B. Jeremic[a], *, D. Vukelic[b], P. M. Todorovic[a], I. Macuzic[a], M. Pantic[a], D. Dzunic[a], and B. Tadic[a]

[a] *Department for Production Engineering, Faculty of Engineering, University of Kragujevac, Kragujevac, 34000 Serbia*

**e-mail: bane@kg.ac.rs*

[b] *Department for Production Engineering, Faculty of Technical Sciences, University of Novi Sad, Novi Sad, 21000 Serbia*

Received November 30, 2012

Abstract—The problem of measuring static friction at high temperatures and low contact pressures is theoretically analyzed, as well as the instruments for the accurate determination of the coefficient of static friction at high temperatures for contact pairs made of steel and bronze. The results of experimental investigation show that at low contact pressure and temperature above 120°C coefficient of static friction dramatically increases. This increase in the coefficient of friction can be of great practical value with regard to the load capacity of contacts where external forces are balanced with friction forces.

Keywords: coefficient of static friction, high temperatures, specific pressure, inclined plane, measuring instrumentation

DOI: 10.3103/S1068366613020037

INTRODUCTION

Depending on the relative velocity of solid bodies in contact, one can discern between the friction of motionless objects and the friction of moving objects [1–4]. The friction that occurs when a body is motionless represents static friction. In order to move the body, one must apply external force to overcome static friction. Static friction grows with an increase in tangential displacement until it reaches a value required to produce the motion of bodies in contact, as shown in Fig. 1.

Although two bodies are motionless on a macroscopic level, there is a microdisplacement, also called "preliminary displacement," which occurs in the contact zone prior to the moving stage. This microdisplacement can reach relatively high values when one of the contact surfaces has small tangential stiffness compared to another contact surface, as is the case with rubber and metal. The principal parameter of static friction is the maximum static force; upon reaching this force, sliding occurs. Then, the friction force decreases and sliding proceeds uniformly.

The coefficient of static friction is determined using the maximum friction force, which must be overcome in order to produce the relative displacement of contact surfaces. The coefficient of friction depends on the normal load, atmosphere, temperature, adsorption films, material, and topography of solids in contact, etc. In general, it can be said that coefficient of static friction increases with an increase in surface roughness parameters [5], while a low coefficient of friction is related to the smooth surfaces [6]. Some authors concluded that certain friction parameters, e.g., skewness and kurtosis, exerted a greater influence on the coefficient of static friction than other parameters [7].

A better understanding of static friction requires knowledge of its generative mechanism, which was the topic of numerous investigations, especially in metal contact pairs [8, 9]. In particular, the authors of [8] studied static friction between a steel ball and an indium block, which concludes that the material starts

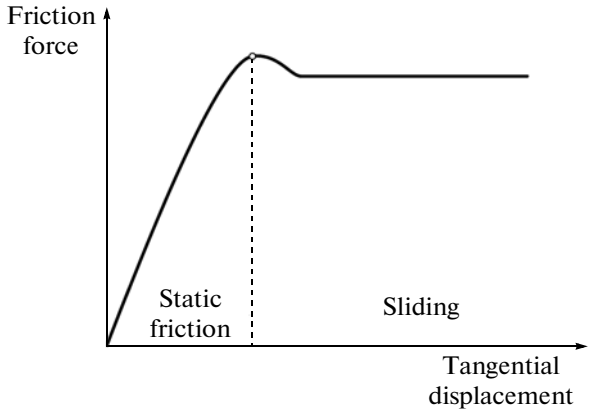

Fig. 1. Friction force vs. tangential displacement.

to flow until the contact surface area is large enough to withstand the load. The displacement due to tangential material flow causes further enlargement of the contact surface area. Due to the constant increase in tangential force, the real contact area grows until the moment when the tangential force surpasses the friction force and sliding begins. At low temperatures, the mechanism of static friction pertains to the creep of asperities in the direction of displacement, while at high temperatures, microwelding occurs and sliding takes place when welding bridges are broken [10].

Experimental studies of static friction have mostly been focused on the moment when the contact makes transition from static friction to sliding. In machinery, this transition is followed by an unwanted stick–slip effect. This effect causes the severe wear of steel contact pairs, which depends strongly on the normal load [11]. The authors of paper [12] investigated static and sliding friction with and without lubrication of steel–steel, steel–aluminum, and aluminum–aluminum contact pairs. They concluded that the steel–aluminum contact pair had the highest coefficient of static friction due to the stick–slip effect, while the steel–steel contact pair exhibited the lowest one. The surface roughness had less influence on the contact of identical materials. The increase in normal load led to an increased coefficient of static friction in the steel–aluminum contact, while in the contact of identical materials, it made no significant impact. The presence of mineral oil in the contact zone had a lower effect on the coefficient of static friction than on the sliding friction.

Friction characteristics of materials at high temperatures were frequently the focus of researchers; however, a very small number of papers studied the coefficient of static friction at high temperatures. The authors of [13] investigated the static and dynamic coefficient of friction using a pin-on-disc tribometer with linear reciprocal displacement. The coefficient of static friction was measured at the moments of the minimum sliding speed, while the dynamic coefficient of friction was measured at the maximum sliding speed. The results showed that the coefficient of static friction was higher than the dynamic coefficient of friction in all experiments, and that it increased with temperature.

The authors of [14] investigated the coefficient of static friction under low normal loads. For normal loads below 100 mg, an average coefficient of static friction increases as the normal load gets lower. For a load range between 100 mg and 1.1 g, the coefficient of static friction practically remained constant and ranged from 0.3 to 0.4. The results indicate that, despite exquisite smoothness, its real contact surface area is still significantly smaller than the nominal one, and the coefficient of static friction still depends on load (this fact is predicted by theory [15]). The tests with solid particles between the contact surfaces have shown that for small loads (<0.9 Pa), the change of the coefficient of static friction is insignificant in the case of both abrasive particles and solid lubricants.

One of the investigation topics was the identification and quantification of the impact of various factors on coefficient of static friction in machining fixtures [16]. The authors attempted to determine the minimum clamping force, which is sufficient to prevent workpiece sliding. They also showed the dependence of the coefficient of static friction on various factors, such as machined surface quality, geometry and size of contact elements, clamping force, presence of lubricant or coolant, and contact pair stiffness. It was concluded that the coefficient of static friction increased with a decrease in body stiffness and is independent of the nominal area of the contact surface.

Static friction was also the focus of theoretical and experimental investigations that suggested useful models pertaining to the layout of roughness patterns on the surface of the elastic bodies and the adsorbed lubricant layer as well as the conditions in which the relative sliding emerges [17–21]. The literature review revealed that the experimental investigations of coefficient of static friction were conducted using various designs of equipment and contact geometry [8, 13, 14, 16, 22–24].

To the best of the authors' knowledge, presently, there are no systematic investigations in the field of coefficient of static friction determination at higher temperatures and low contact pressure. With this in mind, the aim of the work is to improve the known methods for measuring static friction in order to provide reliable tests at high temperatures and low contact pressures.

MATERIALS AND METHODS

The development of a tribometer for measuring the coefficient of static friction at high temperatures and under low contact pressure was faced with a number of physical and technical problems. According to the available literature, there have been no reports on the successful realization of tribometers for the measurement of coefficient of static friction at high temperatures and low contact pressure. The problems are due to the fact that it is difficult to accurately measure very small values of normal load and friction force. Bearing in mind that, for reason of reliability, electronic force sensors must be outside of the high temperature zone, it is necessary to mechanically transmit the signals of small displacements and forces from the high-temperature contact zone to the sensors.

The idea of this study is to improve the method for measuring the coefficient of static friction on an inclined plane. As is well known, the coefficient of static friction represents the ratio between friction force and force that acts normally to the contact surface, where the equilibrium condition on the inclined

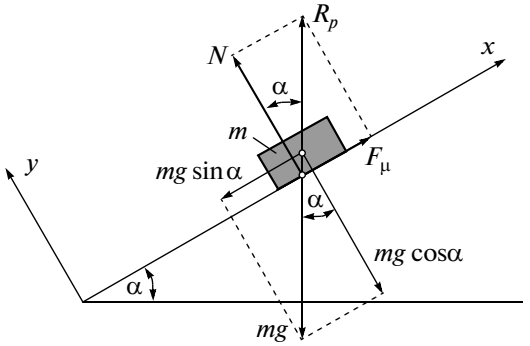

Fig. 2. Equilibrium of body on an inclined plane.

plane is $F_\mu > mg\sin\alpha$ (Fig. 2). In the case of the onset of sliding, we have

$$\mu = \frac{F_\mu}{N} = \frac{mg\sin\alpha}{mg\cos\alpha} = \tan\alpha, \quad (1)$$

where μ is the coefficient of static friction, F_μ is the friction force, m is the body mass, g is the gravitational constant, and α is the angle of plane inclination.

The coefficient of static friction measuring inaccuracy can only be attributed to the inaccuracy of measuring the angle α relative to the horizontal line at the moment when the body makes a transition from the motionless state to displacement. When using some measuring system, if one provides a periodic change of angle α with an accuracy of, e.g., one angle minute 1′ with fairly long time periods Δt, during which the body is resting motionless on the inclined plane, it follows that the measuring inaccuracy is the function of α and the measured coefficient of friction as shown below:

$$\varepsilon = \frac{\tan(\alpha + \Delta\alpha) - \tan\alpha}{\tan\alpha} \cdot 100, [\%], \quad (2)$$

where ε is the relative error and Δα is the angle measuring error. Bearing in mind that the coefficient of friction is $\mu = \tan\alpha$, the diagram in Fig. 3 allows one to determine the relative error ε(μ). The diagram in Fig. 3 clearly shows that, while using an inclined plane to measure a coefficient of static friction of 0.1, the measuring error was just 0.3%. For larger coefficients of friction, the measuring error should be smaller.

A schematic diagram of the device for measuring coefficient of static friction is shown in Fig. 4. As can be seen in the figure, the contact pairs, together with the electric resistance heater and the temperature probe, placed very closely to the contact zone, are ale of rotating for the desired angle, α, relative to the horizontal plane. The measurement of the inclined plane angle is performed mechanically, with an angle reading accuracy of one angle minute. The measuring system is separated from the zone of high temperatures, insulated, balanced with masses m_1 and m_2 and within it there are no components with a temperature above 30°C, even when the contact pairs are heated to

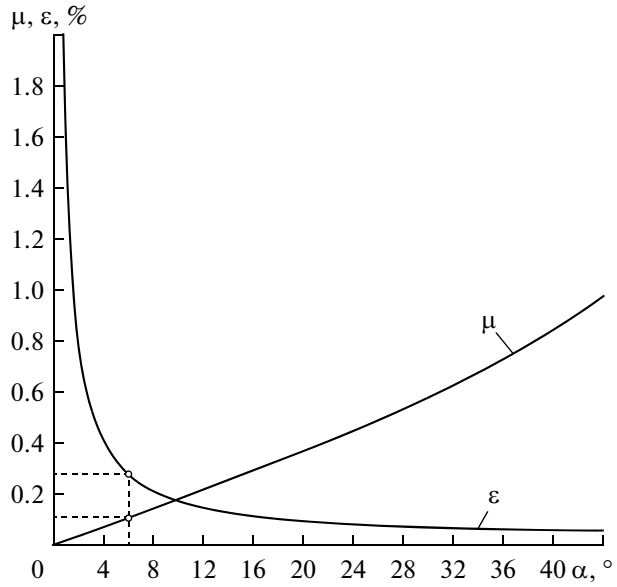

Fig. 3. Graphic representation of relative measuring error of coefficient of friction obtained on an inclined plane.

200°C. Moreover, there are no components within the measuring system that suffer deformation due to mechanical loads.

The photographic images of the proposed device are presented in Fig. 5. It is easy to see that the inclined plane's angular position is regulated manually by turning the graduated angular measurement protractor, the angle-reading accuracy of which is one minute. On the major scale, which is shown in Fig. 5, the angles are etched in degrees; thus, the device allows the inclined plane to be rotated by up to 60°. The device is leveled using the spirit level with an accuracy that exceeds 0.01/200. Based on various geometries, it is possible to simulate various contacts from point to line and surface contacts. A desired contact temperature is set using a thermoregulator.

EXPERIMENTAL INVESTIGATIONS

Experimental investigations were conducted to establish the influence of temperature on the coefficient of static friction. The line contact was simulated between the cylinders and the internal surfaces of the grooves. The photos of the block and test cylinders are shown in Fig. 6.

The test cylinders were made of copper alloy with the following chemical composition: 1.3% Sn, 0.19% P, 98.51% Cu; density 8890 kg/m^3, modulus of elasticity 117 GPa, and Poisson ratio 0.33. The cylinder radii R_v ranged from 2 to 7 mm, while their lengths were equal to 20 mm. Accordingly, the masses of the test cylinders ranged from 2.23 to 27.37 g. The block with the grooves of the following radii: $R_{b1} = 2.5$ mm; $R_{b2} = 5$ mm; $R_{b3} = 6.5$ mm; and $R_{b4} = 8$ mm, was made out

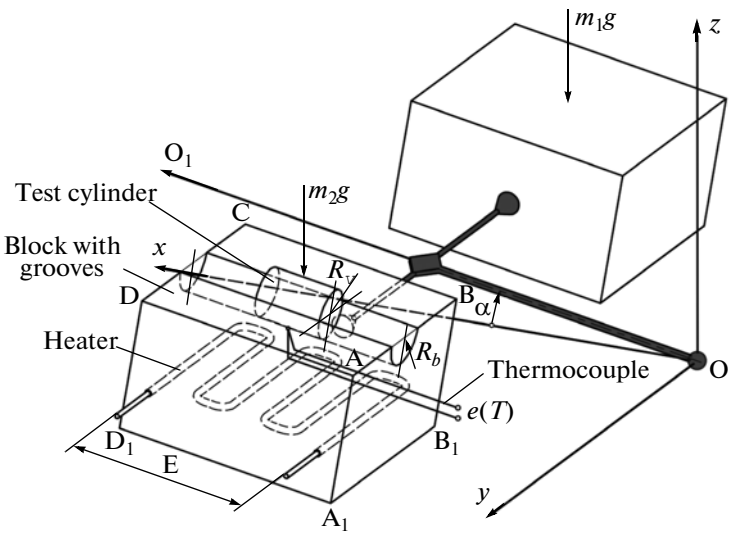

Fig. 4. Schematic diagram of tribometer.

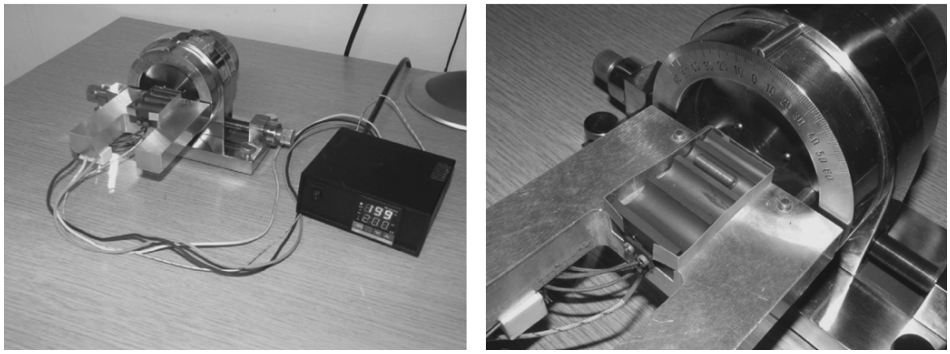

Fig. 5. Photographs of the tribometer.

of chrome alloy steel, 100Cr6 (E52100), with the following chemical composition: 1% C, 0.25% Si, 0.2–0.4% Mn, 1.5% Cr; hardness > 61 *HRC*, modulus of elasticity 203.3 GPa, and Poisson coefficient 0.285. The surface roughness of both contact pairs ranged in the interval of $R_a = 0.8–1$ μm. The experiments were conducted with temperature increments of 20°C, starting from $T_1 = 20$°C, up until $T_2 = 180$°C. Each

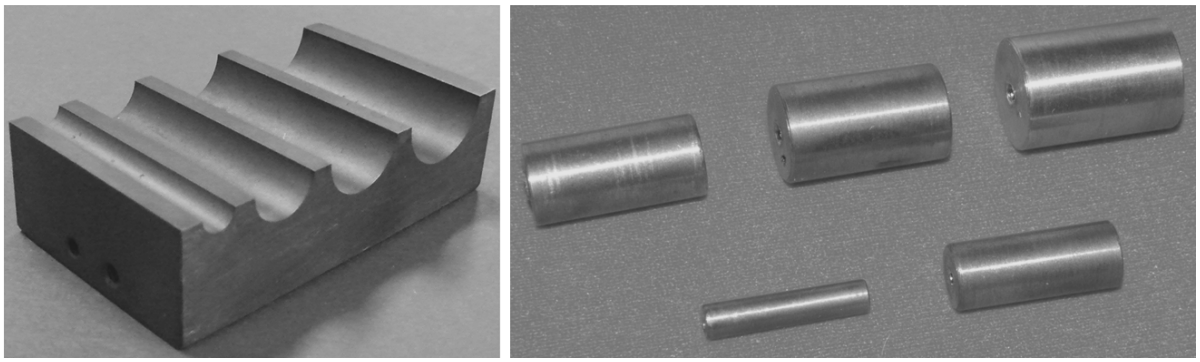

Fig. 6. Photographs of test specimens.

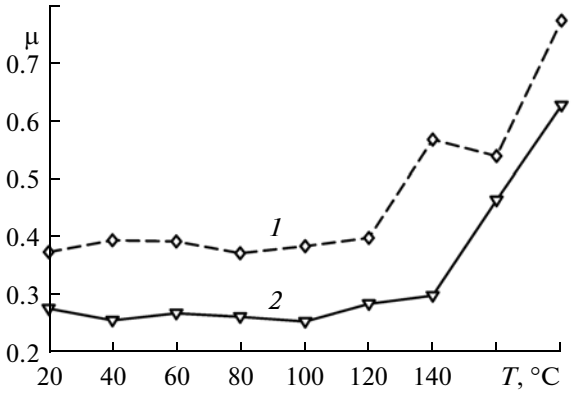

Fig. 7. Static coefficient of friction μ vs. temperature and contact pressure: (*1*) $p = 2.02$ MPa and (*2*) $p = 4.47$ MPa.

measurement was repeated ten times for a total of 1350 independent experiments in order to minimize the influence of random errors.

RESULTS AND DISCUSSION

Using expression $N = mg\cos\alpha$ for $m = 2.23$–27.37 g, and limit values of the angle α, which allow a transition to sliding, the normal contact load was calculated. The values of the normal load ranged from 0.017 to 0.263 N. The cylinders maintained the contact with the groove walls of various radii ($R_{b1} = 2.5$ mm; $R_{b2} = 5$ mm; $R_{b3} = 6.5$ mm; $R_{b4} = 8$ mm) and the contact pressure was calculated based on the theory of elasticity as follows:

$$p = \sqrt{\frac{q}{\nu(k_1 + k_2)}};\ \text{where}\ \nu = \frac{2R_bR_v}{R_b - R_v};$$
$$k_1 = \frac{1-\mu_1^2}{E_1};\quad k_2 = \frac{1-\mu_2^2}{E_2}. \tag{3}$$

Here, p is the contact pressure, q is the load per unit length of cylinder, R_v is the cylinder radius, R_b is the groove radius, μ_1 is the Poisson ratio for cylinder material, μ_2 is the Poisson ratio for block material, E_1 is the elasticity module for cylinder material, and E_2 is the elasticity module for block material. Based on the calculations according to Eq. (3), the theoretical contact pressure varied from 1.89 to 4.70 MPa.

Figure 7 presents a plot of the coefficient of static friction μ versus temperature T, at a contact pressure of $p = 2.02$ MPa, which corresponds to $R_v = 2$ mm and $R_b = 2.5$ mm, and $p = 4.47$ MPa, which corresponds to $R_v = 3$ mm and $R_b = 8$ mm.

Based on the tests, it is clear that the method of inclined plane can be efficiently applied in the experiments at high temperature and low contact pressures. The experiments were performed with small normal loads of 0.017–0.263 N and theoretical contact pressures in the interval of 1.89–4.70 MPa.

It should be noted that the real contact pressure obtained for small normal loads probably deviates from the calculated pressure, but based on the tests, it can be concluded that temperature has a pronounced influence on the coefficient of static friction. For example, the temperature variation at 20–180°C results in the almost triple coefficient of static friction. These large changes in the coefficient of static friction are obviously the result of thermal influence on the contact pair material and/or surface films, e.g., water and organic contaminants, which can serve a lubricant [18]. The coefficient of static friction remains relatively constant up until a temperature of 120°C, but it seems that temperatures above 120°C causes changes of tribological properties in the surface layers of the contact pairs and/or the adsorbed films.

Based on the diagram shown in Fig. 7, it follows that, over the entire temperature range, lower contact pressure p corresponds to a higher coefficient of static friction μ and vice versa. This proves that, even at low contact pressures and high temperatures, the coefficient of static friction depends on contact pressure, which complies with the results obtained under different experimental conditions [14, 23, 24]. It should be noted that the increase in the dispersion of the coefficient of friction, which is observed as the oscillation around the basic trend line, quite probably results to at least some extent from inevitable differences in contact pair topographies. It has already been mentioned that, prior to the experiment, the roughness of contact pairs was made approximately equal to $R_a = 0.8$–1.0 μm. However, the average arithmetic roughness is not the only parameter of the surface pattern; there are many other parameters that contribute to the effect of roughness and texture on friction [25].

CONCLUSIONS

The developed device for measuring the coefficient of static friction at high temperatures and small contact loads, which employs the inclined plane principle, is designed to allow the very accurate determination of the coefficient of static friction. The inclination angle readout error is less than 1 min, which means that the measuring inaccuracy of the coefficient of static friction can be disregarded for practical purposes. This is especially true when measuring it at higher temperatures, i.e., for higher static sliding coefficients of friction.

The results of measuring the coefficient of static friction at high temperatures and small contact loads (low contact pressures and small normal load) indicate that temperature and contact pressure significantly impact the value and dispersion of the coefficient of friction.

There are numerous areas of engineering, especially mechanical engineering, where external static or dynamic loads are balanced by friction forces. Accordingly, a significant increase in the coefficient of static

friction at temperatures within 120–180°C, under small specific pressures, can have important industrial applications with regard to higher loads of tangentially loaded contact interfaces where external forces are in equilibrium with the friction forces.

Future investigations should be directed towards the more accurate determination of the reasons for temperature effect, in particular at controlled humidity, as well as a more detailed evaluation of the roughness and texture effect on static friction.

DESIGNATIONS

F_μ—friction force; μ—coefficient of static friction; m—body mass; g—gravitational constant; α—angle of plane inclination; ε—relative error; $\Delta\alpha$—angle measuring error; p—contact pressure; q—load per unit length of cylinder; R_v—cylinder radius; R_b—groove curve radius; μ_1—Poisson ratio for cylinder material; μ_2—Poisson ratio for block material; E_1—elasticity module for cylinder material; E_2—elasticity module for block material; T—temperature; R_a—surface roughness.

REFERENCES

1. Kragel'skii, I.V., Dobychin, M.N., and Kombalov, V.S., *Osnovy raschetov na trenie i iznos* (Foundations of Calculation on Friction and Wear), Moscow: Mashinostroenie, 1976.
2. Maksak, V.V., *Predvaritel'noe smeshchenie i kontaktnaya zhestkost'* (Preliminary Displacement and Contact Hardness), Moscow: Nauka, 1975.
3. Myshkin, N.K. and Petrokovets, M.I., *Trenie, smazka, iznos* (Friction, Lubricating, Wear), Moscow: Fizmatlit, 2007.
4. Blau, P., The significance and use of the friction coefficient, *Tribol. Int.*, 2001, vol. 34, pp. 585–591.
5. Ivkovic, B., Durdjanovic, M., and Stamenkovic, D., The Influence of the contact surface roughness on the static friction coefficient, *Tribol. Ind.,* 2000, vol. 22, nos. 3–4, pp. 41–44.
6. Muller, U. and Hauert, R., Investigations of the coefficient of static friction diamond-like carbon films, *Surf. Coat. Technol.,* 2003, vol. 174–175, pp. 421–426.
7. Tayebi, N. and Polycarpou, A.A., Modeling the effect of skewness and kurtosis on the static friction coefficient of rough surfaces, *Tribol. Int.*, 2004, vol. 37, pp. 491–505.
8. McFarlane, J.S. and Tabor, D., Relation between friction and adhesion, *Proc. Roy. Soc. Ser. A, Math. Phys. Sci.*, 1950, vol. 202, pp. 244–253.
9. Chang, W.R., Etsion, I., and Bogy, D.B., Static friction coefficient model for metallic rough surfaces, *J. Tribol.*, 1988, vol. 110, pp. 57–63.
10. Galligan, J.M. and McCullough, P., On the nature of static friction, *Wear*, 1985, vol. 105, pp. 337–340.
11. Myshkin, N.K., Kim, C.K., and Petrokovets, M.I., *Introduction to Tribology*, Seoul: CMG Publishers, 1997.
12. Hwang, D.H. and Zum, G.K.H., Transition from static to kinetic friction of unlubricated or oil lubricated steel/steel, steel/ceramic and ceramic/ceramic pairs, *Wear*, 2003, vol. 255, pp. 365–375.
13. Kumar, H., Ramakrishnan, V., Albert, S.K., Meikandamurthy, C., Tata, B.V.R., and Bhaduri, A.K., High temperature wear and friction behavior of 15Cr–15Ni–2Mo titanium-modified austenitic stainless steel in liquid sodium, *Wear*, 2010, vol. 270, pp. 1–4.
14. Dunkin, E.J. and Kim, E.D., Measurement of static friction coefficient between flat surfaces, *Wear*, 1996, vol. 193, pp. 186–192.
15. Chizhik, S.A., Gorbunov, V.V., and Myshkin, N.K., Analysis of molecular scale roughness effect on contact of solids based on computer modeling, *Precis. Eng.,* 1995, vol. 17, pp. 186–191.
16. Xie, W., De Meter, E.C., and Trethewey, M.W., An experimental evaluation of coefficients of static friction of common workpiece-fixture element pairs, *Int. J. Mach. Tools Manuf.*, 2000, vol. 40, pp. 467–488.
17. Sokoloff, J.B., Static friction between elastic solids due to random asperities, *Phys. Rev. Lett.*, 2001, vol. 86, pp. 3312–3315.
18. Kato, S., Marui, E., Kobayashi, A., and Senda, S., The influence of lubricants on static friction characteristics under boundary lubrication, *J. Tribol.*, 1985, vol. 107, pp. 188–194.
19. Ruff, A.W. and Myshkin, N.K., Lubricated wear behavior of composition-modulated nickel–copper coatings, *J. Tribol. (Trans.(ASME)*, 1989, vol. 111, pp. 156–160.
20. Muser, M.H. and Robbins, M.O., Conditions for static friction between flat crystalline surfaces, *Phys. Rev. B: Condens. Matter Mater. Phys.*, 2000, vol. 61, pp. 2335–2342.
21. Reiter, G., Demirel, A.L., Peanasky, J., Cai, L., and Granick, S., What determines static friction and controls the transition to sliding, *Tribol. Lett.*, 1995, vol. 1, pp. 1–12.
22. Seo, N.J., Armstrong, T.J., and Drinkau, P., A comparison of two methods of measuring static coefficient of friction at low normal forces, *Ergonomics*, 2009, vol. 52, pp. 121–135.
23. Aleksandrovic, S., Nedeljkovic, B., Stefanovic, M., Milosavljevic, D., and Lazic, V., Tribological properties of steel and Al-alloys sheet metals intended for deep drawing, *Tribol. Ind.*, 2009, vol. 31, pp. 11–16.
24. Marjanovic, N., Ivkovic, B., Stojanovic, B., and Blagojevic, M., Disk on disk test of gear pair power losses, *Tribol. Ind.*, 2010, vol. 32, pp. 10–16.
25. Myshkin, N.K., Grigoriev, A.Y., and Kholodilov, O.V., Quantitative analysis of surface topography using scanning electron microscopy, *Wear*, 1992, vol. 153, pp. 119–133.

Translated by I. Kekukh